Soil Moisture and Hydrology Projections of the Permafrost Region: A Model Intercomparison

Christian G. Andresen[1,2], David M. Lawrence[3], Cathy J. Wilson[1], A. David McGuire[4], Charles Koven[5], Kevin Schaefer[6], Elchin Jafarov[6,1], Shushi Peng [7], Xiaodong Chen[8], Isabelle Gouttevin[9,10], Eleanor Burke[11], Sarah Chadburn[12], Duoying Ji[13], Guangsheng Chen[14], Daniel Hayes[15], Wenxin Zhang[16,17]

[1]Earth and Environmental Science Division, Los Alamos National Laboratory, Los Alamos, New Mexico, USA
[2]Geography Department, University of Wisconsin Madison, Madison, Wisconsin, USA
[3]National Center for Atmospheric Research, Boulder, Colorado, USA
[4]Institute of Arctic Biology, University of Alaska Fairbanks, Fairbanks, Alaska, USA
[5]Climate and Ecosystem Sciences Division, Lawrence Berkeley National Lab, Berkeley, CA, USA
[6]Institute of Arctic Alpine Research, University of Colorado Boulder, Boulder, Colorado, USA
[7] UJF–Grenoble 1/CNRS, Laboratoire de Glaciologie et Géophysique de l'Environnement (LGGE), Grenoble, France
[8]Department of Civil and Environmental Engineering, University of Washington, Seattle, Washington, USA
[9]IRSTEA-HHLY, Lyon, France.
[10]IRSTEA-ETNA, Grenoble, France.
[11]Met Office Hadley Centre, UK
[12]School of Earth and Environment, University of Leeds, UK
[13]College of Global Change and Earth System Science, Beijing Normal University, China
[14]Environmental Sciences Division, Oak Ridge National Laboratory, Oak Ridge, Tennessee, USA
[15] School of Forest Resources, University of Maine, Maine, USA
[16] Department of Physical Geography and Ecosystem Science, Lund University, Lund, Sweden
[17]Center for Permafrost (CENPERM), Department of Geosciences and Natural Resource Management, University of Copenhagen, Denmark

Correspondence to: Christian G. Andresen (candresen@wisc.edu)

Abstract. This study investigates and compares soil moisture and hydrology projections of broadly-used land models with permafrost processes and highlights the causes and impacts of permafrost zone soil moisture projections. Climate models project warmer temperatures and increases in precipitation (P) which will intensify evapotranspiration (ET) and runoff in land models. However, this study shows that most models project a long-term drying of the surface soil (0-20cm) for the permafrost region despite increases in the net air-surface water flux (P-ET). Drying is generally explained by infiltration of moisture to deeper soil layers as the active layer deepens or permafrost thaws completely. Although most models agree on drying, the projections vary strongly in magnitude and spatial pattern. Land-models tend to agree with decadal runoff trends but underestimate runoff volume when compared to gauge data across the major Arctic river basins, potentially indicating model structural limitations. Coordinated efforts to address the ongoing challenges presented in this study will help reduce uncertainty in our capability to predict the future Arctic hydrological state and associated land-atmosphere biogeochemical processes across spatial and temporal scales.

1. Introduction

Hydrology plays a fundamental role in permafrost landscapes by modulating complex interactions among biogeochemical cycling (Frey and Mcclelland, 2009; Newman et al., 2015; Throckmorton et al., 2015), geomorphology (Grosse et al., 2013; Kanevskiy et al., 2017; Lara et al., 2015; Liljedahl et al., 2016) and ecosystem structure and function (Andresen et al., 2017; Avis et al., 2011; Oberbauer et al., 2007). Permafrost has a strong influence on hydrology by controlling surface and sub-surface distribution,

storage, drainage and routing of water. Permafrost prevents vertical water flow which often leads to saturated soil conditions in continuous permafrost while confining subsurface flow through perennially-unfrozen zones (a.k.a. taliks) in discontinuous permafrost (Jafarov et al., 2018; Walvoord and Kurylyk, 2016). However, with the observed (Streletskiy et al., 2008) and predicted (Slater and Lawrence, 2013) thawing of permafrost, there is a large uncertainty in the future hydrological state of permafrost landscapes and in the associated responses such as the permafrost carbon-climate feedback.

The timing and magnitude of the permafrost carbon-climate feedback is, in part, governed by changes in surface hydrology, through the regulation by soil moisture of the form of carbon emissions from thawing labile soils and microbial decomposition as either CO_2 or CH_4 (Koven et al., 2015; Schädel et al., 2016; Schaefer et al., 2011). The impact of soil moisture changes on the permafrost-carbon feedback could be significant. Lawrence et al. (2015) found that the impact of the soil drying projected in simulations with the Community Land Model decreased the overall Global Warming Potential of the permafrost carbon-climate feedback by 50%. This decrease was attributed to a much slower increase in CH_4 emissions if surface soils dry, which is partially compensated for by a stronger increase in CO_2 emissions under drier soil conditions.

Earth System Models project an intensification of the hydrological cycle characterized by a general increase in the magnitude of water fluxes (e.g. precipitation, evapotranspiration and runoff) in northern latitudes (Rawlins et al., 2010; Swenson et al., 2012). In addition, intensification of the hydrological cycle is likely to modify the spatial and temporal patterns of water in the landscape. However, the spatial variability, timing, and reasons for future changes in hydrology in terrestrial landscapes in the Arctic are unclear and variability in projections of these features by current terrestrial hydrology applied in the Arctic have not been well documented. Therefore, there is an urgent need to assess and better understand hydrology simulations in land models and how differences in process representation affect projections of permafrost landscapes.

Upgrades in permafrost representation such as freeze and thaw processes in the land component of Earth System Models have improved understanding of the evolution of hydrology in high northern latitudes. Particularly, soil thermal dynamics and active layer hydrology upgrades include the effects of unfrozen water on phase change, insulation by snow (Peng et al., 2015), organic soils (Jafarov, E. and Schaefer, 2016; Lawrence et al., 2008) and hydraulic properties of frozen soils (Swenson et al., 2012). Nonetheless, large discrepancies in projections remain as the current generation of models substantially differ in soil thermal dynamics (e.g. Peng *et al* 2015, Wang *et al* 2016). In particular, variability among current models' simulations of the impact of permafrost thaw on soil water and hydrological states is not well documented. Therefore, in this study we analyze the output of a collection of widely-used "permafrost-enabled" land models. These models participated in the Permafrost Carbon Network Model Intercomparison Project (PCN-MIP) (McGuire et al., 2018, 2016) and contained the state-of the art representations of soil thermal dynamics in high latitudes at that time. In particular, we assess how changes in active layer thickness and permafrost thaw influence near-surface soil moisture and hydrology projections under climate change. In addition, we provide comments on the main gaps and challenges in permafrost hydrology simulations and highlight the potential implications for the permafrost carbon-climate feedback.

2. Methods

2.1 Models and Simulation Protocol

This study assesses a collection of terrestrial simulations from models that participated in the PCN-MIP (McGuire et al., 2018, 2016) (Table 1). The analysis presented here is unique as it focuses on the hydrological component of these models. Table 2 describes the main hydrological characteristics for each model. Additional details on participating models regarding soil thermal properties, snow, soil carbon and forcing trends can be found in previous PCN-MIP studies (e.g. McGuire *et al* 2016, Koven *et al* 2015, Wang *et al* 2016, Peng *et al* 2015). It is important to note that the versions of the models presented in this study are from McGuire *et al* (2016, 2018) and some additional improvements to individual models may have been made since then.

The simulation protocol is described in detail in *McGuire et al.*, (2016, 2018). In brief, models' simulations were conducted from 1960 to 2299, partitioned by historic (1960-2009) and future simulations (2010-2299), where future simulations were forced with a common projected climate derived from a fully coupled climate model simulation (CCSM4) (Gent et al., 2011). Historic atmospheric forcing datasets (Table 1) (e.g. climate, atmospheric CO_2, N deposition, disturbance, etc.) and spin-up time were specific to each modeling group. The horizontal resolution (0.5° – 1.25°) and soil hydrological column configurations (depths ranging from 2 to 47m and 3 to 30 soil layers) also vary across models (Figure 1). We focus on results from simulations forced with climate and CO_2 from the Representative Concentration Pathway (RCP) 8.5 scenario, which represents unmitigated, "business as usual" emissions of greenhouse gases. Future simulations were calculated from monthly CCSM4 (Gent et al., 2011) climate anomalies for the Representative Concentration Pathway (RCP 8.5, 2006-2100) and the Extension Concentration Pathway (ECP 8.5, 2101-2299) scenarios, relative to repeating (1996-2005) forcing atmospheric datasets from the different modeling groups (Table 1).

The PCN model intercomparison uses the output from a single Earth System model climate projection and was motivated by a desire to keep the experimental design simple and computationally tractable. Clearly, using just one climate projection does not allow us to explore the impact of the broad range of potential climate outcomes that are seen across the CMIP5 models. Instead, the PCN suite of simulations allows for a relatively controlled analysis of the spread of model responses to a single representative climate trajectory. The selection of CCSM4 as the climate projection model was motivated partly by convenience and also because it was one of the only models that had been run out to the year 2300 at the time of the PCN experiments. Further, as noted in McGuire et al. (2018), CCSM4 late 20th century climate biases in the Arctic were among the lowest across the CMIP5 model archive. It should be noted that the use of a single climate projection means that the results presented here should be viewed as indicative of just one possible permafrost hydrologic trajectory. As we will show, even under this single climate trajectory, the range of hydrologic responses in the models are broad, indicating high structural uncertainty across models with respect to this particular aspect of the Arctic system response to global climate change.

2.2 Permafrost and Hydrology Variables Analyzed

Our analysis focused on the permafrost regions in the Northern Hemisphere north of 45^0N. This qualitative hydrology comparison was based on the full permafrost domain for each model rather than a common subset among models in order to fully portray the overall changes in permafrost hydrology for participating models. For each model, we define a grid cell as containing near-surface permafrost based on soil temperature where the annual monthly maximum active layer thickness (ALT) is at or less than the 3m depth layer depending on the model soil configuration (Figure 1) (McGuire et al., 2016; Slater and Lawrence, 2013). We calculated the depth of max ALT by identifying the underlying annual permafrost table depth of continuous monthly temperatures <273.15°k in the top 3 meters or equivalent soil layer depth (Figure 1). Models with a soil configuration at 3 meters or less (UWVIC, CoLM, JULES, TEM) follow the same calculation with an exemption for their bottom depth, where soil depth temperature threshold of <273.5°k was applied to be considered as permafrost, this was based on soil temperature trends observed for models with deeper soil depths greater than 3 meters and allows models to have a ALT of 3 meters when soil configuration is limiting. We assessed how permafrost changes affect near-surface soil moisture, defined here as the soil water content (kg/m^2) of the 0-20 cm soil layer. We focused on the top 20 cm of the soil column due to its relevance to near-surface biogeochemical processes. We added the weighted fractions for each depth interval to calculate near-surface soil moisture (0-20cm) to account for the differences in the vertical resolution of the soil grid cells among models (Figure 1). To better understand the causes and consequences of changes in soil moisture, we examined several principal hydrology variables including evapotranspiration (ET), runoff (R; surface and sub-surface) and precipitation (P; snow and rain). Representation of ET, R and soil hydrology varies across participating models and are summarized in table 2.

We compared model simulations with long-term (1970-1999) mean monthly discharge data from Dai *et al* (2009). We computed model total annual discharge (sum of surface and subsurface runoff) for the main river basins in the permafrost region of North America (Mackenzie, Yukon) and Russia (Yenisei, Lena). In particular, we compared (i) annual runoff anomalies, (ii) correlation coefficients and (iii) distributions of annual discharge between gauge data and models' simulations for the 30-year period of 1970-1999. Gauge stations from major permafrost river basins used for simulation comparison include (i) Arctic Red, Canada (67.46^0N, 133.74^0W) for Mackenzie River, (ii) Pilot Station, Alaska (61.93^0N 162.88^0W) for Yukon River, (iii) Igarka, Russia (67.43^0N, 86.48^0E) for Yenisey River and (iv) Kusur, Russia (70.68^0N, 127.39^0E) for Lena River.

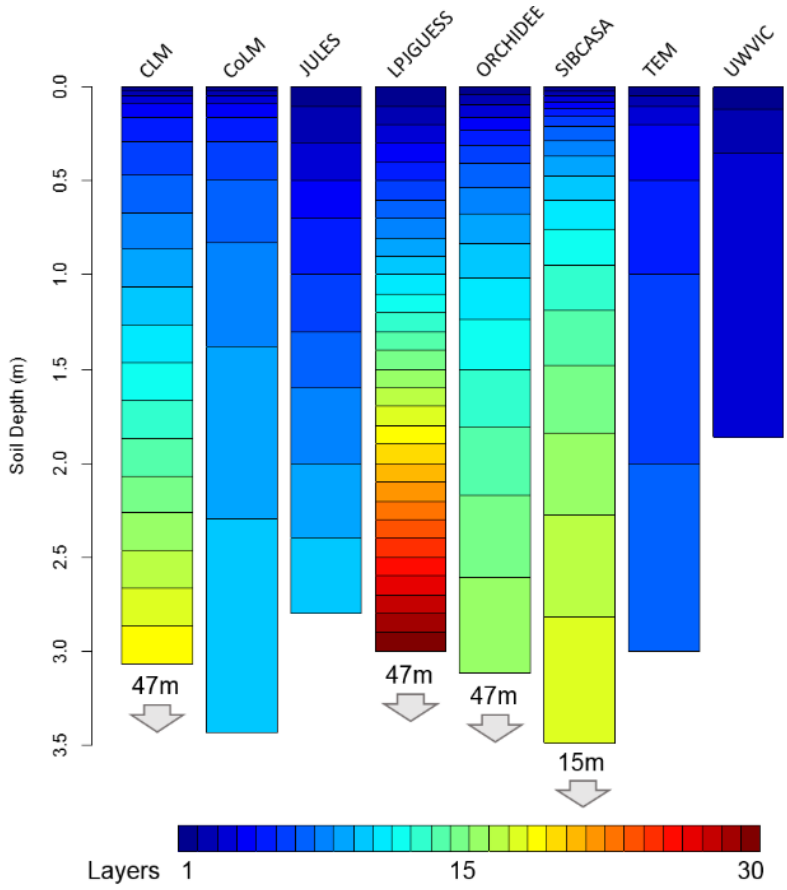

Figure 1. Soil hydrologically-active column configuration for each participating model. Numbers and arrows indicate full soil configuration of non-hydrologically active bedrock layers. Colors represent the number of layers.

Table 1. Models description and driving datasets.

Model	Full Name	Climate Forcing Dataset	Model Reference	Short-Wave radiation[a]	Long-Wave Radiation[a]	Vapor Pressure[a]
CLM 4.5	Community Land Model v4.5	CRUNCEP4[b]	Oleson *et al* (2013)	Yes	Yes[c]	Yes
CoLM	Common Land Model	Princeton[d]	Dai *et al* (2003), Ji *et al* (2014)	Yes	Yes	Yes
JULES	Joint UK Land Environment Simulator model	WATCH (1901-2001)[e]	Best *et al* (2011)	Yes	Yes	Yes
ORCHIDEE-IPSL	Organising Carbon and Hydrology In Dynamic Ecosystems	WATCH (1901-1978)[e]	Gouttevin, I. *et al* (2012), Koven *et al* (2009), Krinner *et al* (2005)	Yes	Yes	Yes

LPJGUESS	Lund-Postdam-Jena dynamic global veg model	CRU TS 3.1[f]	Gerten *et al* (2004), Wania *et al* (2009b, 2009a)	Yes	No	No
SiBCASA	Simple Biosphere/Carnegie-Ames-Standford Approach model	CRUNCEP4[b]	Schaefer *et al* (2011), Bonan (1996), Jafarov, E. and Schaefer (2016)	Yes	Yes	Yes
TEM604	Terrestrial Ecosystem Model	CRUNCEP4[b]	Hayes *et al* (2014, 2011)	Yes	No	No
UW-VIC	Univ. of Washignton Variable Infiltration Capacity model	CRU[f], Udel[h]	Bohn *et al* (2013)	Internally calculated	Internally calculated	Yes

[a]Simulations driven by temporal variability

[b]Viovy and Ciais (http://dods.extra.cea.fr/)

[c]Long-wave dataset not from CRUNCEPT4

[d]Sheffield *et al* (2006) (http://hydrology.princeton.edu/data.pgf.php)

[e]http://www.eu-watch.org/gfx_content/documents/README-WFDEI.pdf

[f]Harris *et al* (2014), University of East Anglia Climate Research Unit (2013)

[g]Mitchell and Jones (2005) for temperature

[h]Willmott and Matsuura (2001) for wind speed and precipitation with corrections (see Bohn et al. 2013).

Table 2. Hydrology and soil thermal characteristics of participating models.

	Hydrology								Soil Thermal Properties			
Model	Evapotranspiration approach	Root water uptake	Infiltration	Water table	Soil Water Storage and Transmission	Groundwater Dynamics	Soil-ice impact	Snow	Soil thermal dynamics approach	Unfrozen Water effects on Phase Change	Moss insulation	Organic soil insulation
CLM 4.5	Sum of canopy evaporation, transpiration, and soil evaporation	Macroscopic approach	Saturation-excess runoff $F_{sat}=f(z_{wt})$	Niu et al. (2007); perched water table possible if ice layer present	Richard's equation (Clapp Hornberger functions)	Base flow from TOPMODEL concepts, unconfined aquifer (Niu et al. 2007)	Impacts hydrologic properties through power-law ice impedance (Swenson et al., 2012)	Multi-layer dynamic (5 max)	Multi-layer Finite Difference Heat Diffusion	Yes	No	Yes
CoLM	BATS and Philip's (1957)	Macroscopic approach	Saturation-excess runoff $F_{sat}=f(z_{wt})$	Simple TOPMODEL	Richard's equation (Clapp Hornberger functions)	Base flow from TOPMODEL	Impacts hydrologic properties through power-law ice impedance	Multi-layer dynamic (5 max)	Multi-layer Finite Difference Heat Diffusion	No	No	No
JULES	Sum of ET, soil evaporation and moisture storages (e.g. lakes, urban) minus surface resistance	Macroscopic approach	Saturation-excess runoff $F_{sat}=f(z_{wt})$ or $F_{sat}=f(\theta)$	TOPMODEL or Probability Distribution Model	Richard's equation (Clapp Hornberger/van Genuchten functions)	Base flow from TOPMODEL	Hydraulic conductivity and suction determined by unfrozen water content (Brooks and Corey functions)	Multi-layer dynamic (3 max)	Multi-layer Finite Difference Heat Diffusion	Yes	No	No
ORCHIDEE-IPSL	Sum of bare soil, interception loss and plant transpiration for different veg PFTs in grid cell.	Macroscopic approach, water uptake different among cell veg PFTs (de Rosnay and Polcher, 1998)	Saturation-excess runoff $F_{sat}=f(\theta)$	TOPMODEL	Richard's equation (van Genuchten functions)	None	"Drying=Freezing" approximation (Gouttevin et al 2012)	Multi-layer dynamic (7 max)	1D Fourier Solution	Yes	No	Yes
LPJ-GUESS	Sum of Interception loss, plant transpiration and evaporation from soil. Gerten et al (2004)	Fractional water uptake from different soil layers according to prescribed root distribution. (Wania et al., 2009a,b)	Depends on soil moisture and layer thickness. Declines exponentially with soil moisture	Uniform, and only for wetland grid cell (Wania et al., 2009a,b)	Analog to Darcy's Law, percolation rate depends on soil texture conductivity and soil wetness (Haxeline and Prentice, 1996).	Base flow is based on the exponential function to estimate percolation rate	Impacts hydrologic properties through power-law ice impedance	Multi-layer dynamic (3 max)	Multi-layer Finite Difference Heat Diffusion	No	No	No
SiBCASA	Sum of ground evaporation, surface dew, canopy ET and canopy dew (Bonan, 1996)	Macroscopic approach	Infiltration approach in non-saturated porous media described by Darcy's law	Niu et al. (2007); perched water table possible if ice layer present	Richard's equation (Clapp Hornberger functions)	Base flow from TOPMODEL concepts, unconfined aquifer (Niu et al. 2007)	Impacts hydrologic properties through power-law ice impedance	Multi-layer dynamic (5 max)	Multi-layer Finite Difference Heat Diffusion	Yes	No	Yes
TEM-604	Jenson-Haise potential ET (PET, Jenson and Haise 1963). Actual ET is calculated based on PET, water availability and leaf mass.	Based on the proportion of actual ET to potential ET	Field capacity-excess runoff (Thornthwaite and Mather 1957)	none	one-layer bucket	none	none	Multi-layer dynamic (9 max)	Multi-layer Finite Difference Heat Diffusion	No	Yes	No
UW-VIC	Sum of canopy interception, veg. transpiration and soil evaporation (Liang et al. 1994)	Based on reference ET and soil wilting point	Saturation-excess runoff $F_{sat}=f(\theta)$	Microtopography	From infiltration rate and infiltration shape parameter (Liang et al. 1994). No lateral flow between model grids	Base flow from Arno model conceptualization (Francini and Pacciani 1991)	Impacts hydrologic properties through power-law ice impedance	Bulk-layer dynamic (2 max)	Multi-layer Finite Difference Solution	Yes	No	Yes

2. Results

3.1 Soil Moisture

Air temperature forcing from greenhouse-gas emissions shows an increase of ~15ºC in the permafrost domain over the simulation period (Figure 2a). With increases in air temperature, models project an ensemble mean decrease of ~13 million km^2 (91%) of the permafrost domain by 2299 (Figure 2b). Coincident with these changes, most models projected a long-term drying of the near-surface soils when averaged over the permafrost landscape (Figure 2c). However, the simulations diverged greatly with respect to both the permafrost-domain average soil moisture response and their associated spatial patterns (Figure 2c, 3). The models' ensemble mean indicated a change of -10% in near-surface soil moisture for the permafrost region by year 2299, but the spread across models was large. COLM and LPJGUESS simulate an increase in soil moisture of 10% and 48%, respectively. CLM, JULES, TEM6 and UWVIC exhibit qualitatively similar decreasing trends in soil moisture ranging between -5% and -20%. SIBCASA and ORCHIDEE projected a large soil moisture change of approximately -50% by 2299. Spatially,

models show diverse wetting and drying patterns and magnitudes across the permafrost zone (Figure 3). Several models tend to get wetter in the colder northern permafrost zones and are more susceptible to drying along the southern permafrost margin. Other models, such as TEM6 and UWVIC show the opposite pattern with drying more common in the northern part of the permafrost domain.

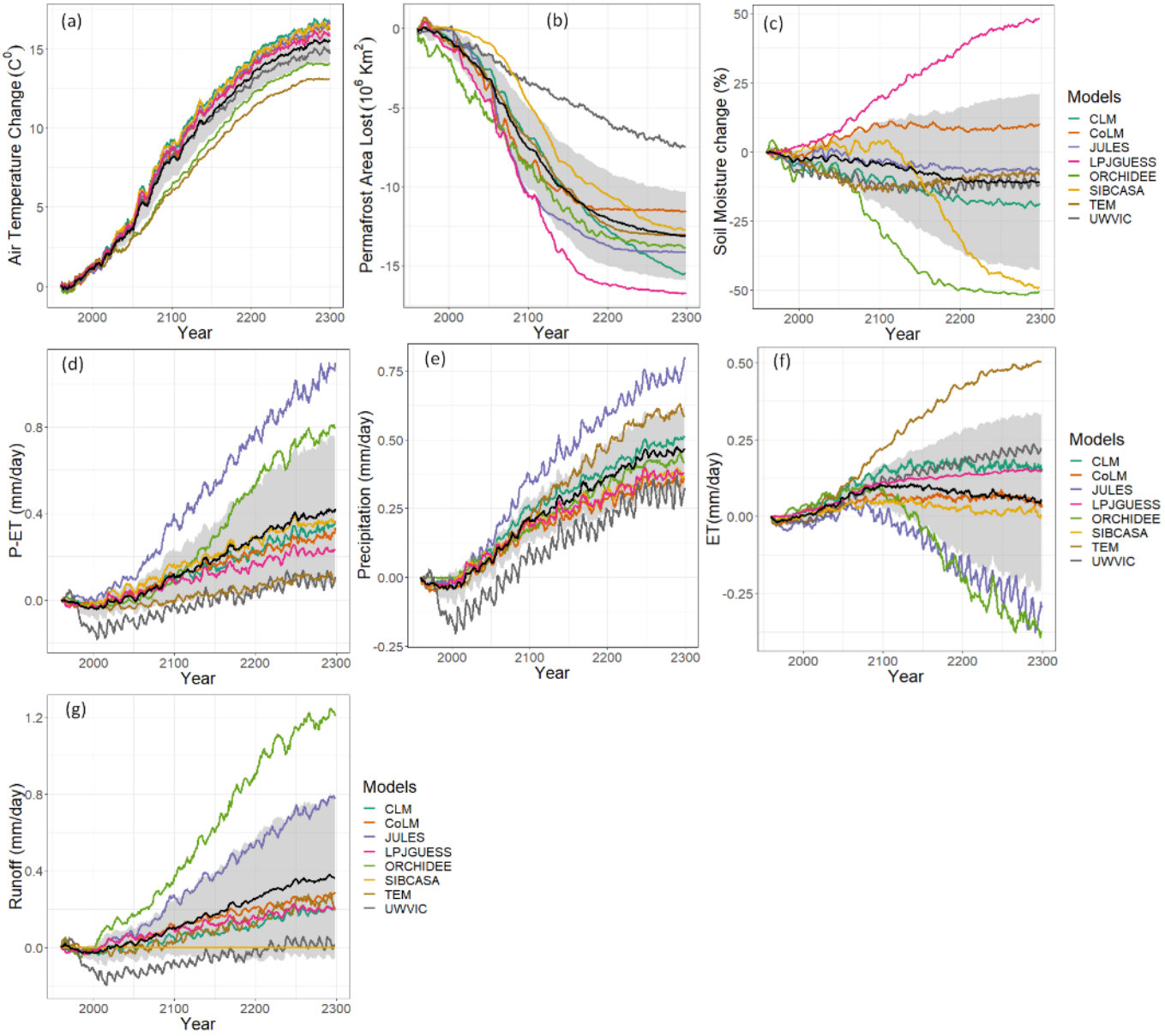

Figure 2. Simulated annual mean changes in air temperature, near-surface permafrost area, near-surface soil moisture and hydrology variables relative to 1960 (RCP 8.5). Annual mean is computed from monthly output values. The black line represents the models' ensemble mean and the gray area is the ensemble standard deviation. Figures d, e, f, and g are represented as change from 1960 values. Time series are smoothed with a 7-year running mean for clarity and calculated over the initial permafrost domain of each model in 1960 for latitude >45^{0}N.

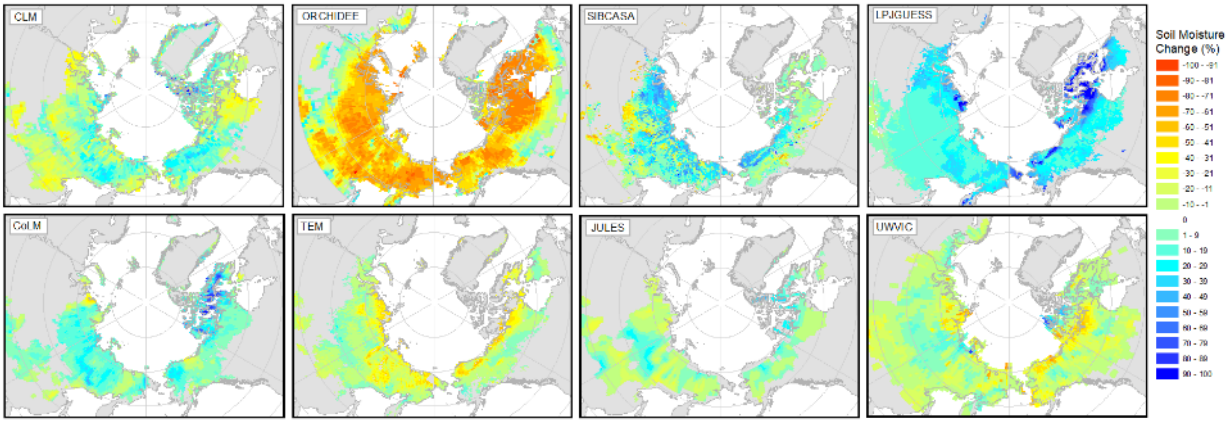

Figure 3. Spatial variability of projected changes in surface soil moisture (%) among models. Depicted changes are calculated as the difference between the 2071 to 2100 average and the 1960 to 1989 average. Colored area represents the initial simulated permafrost domain of 1960 for each model.

3.2 Drivers of Soil Moisture Change

To understand why models projected upper soil drying despite increases in the net precipitation (P-ET) into the soil, we examined whether or not increases in active layer thickness (ALT) and/or complete thaw of near-surface permafrost could be related to surface soil drying of the top 0-20cm ALT. We observed a general significant negative correlation in most models (except SIBCASA, LPJGUESS) where cells with greater increases in active layer thickness have greater drying (decrease) in near-surface soil moisture (Figure 4). However, there is a large spread between soil moisture and ALT changes (Figure 4). This spread may be influenced by many interacting factors that can be difficult to assess directly and are out of the scope of this study. In addition, the coarse soil column discretization in UWVIC limited this analysis for this model (Figure 1). However, most models show some indication that as the active layer deepens, soils tend to get drier at the surface.

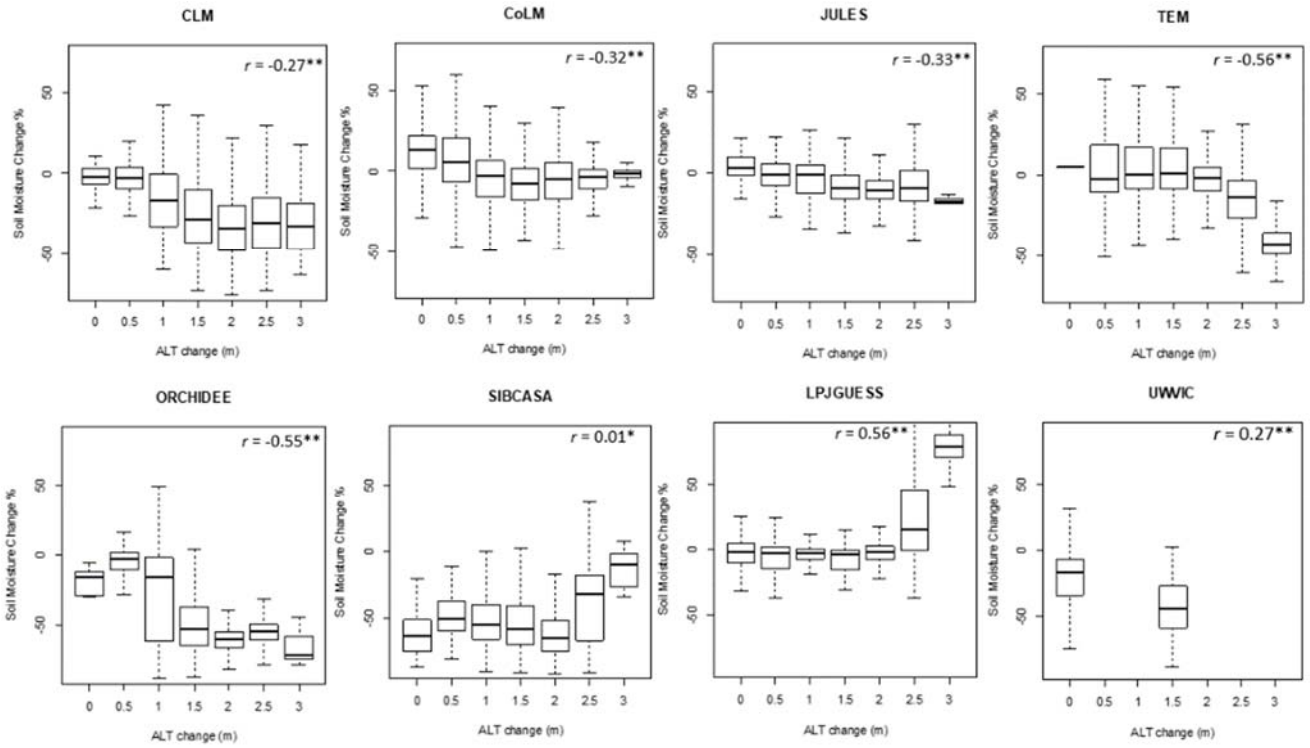

Figure 4. Responses of August near-surface (0-20cm) soil moisture to ALT changes. Each box represents a range of ±0.25m of ALT change. ALT and soil moisture change are calculated as the 2290-2299 average minus the 1960-1989 average for cells in the initial permafrost domain of 1960. For cells where ALT exceeded 3 meters (no permafrost) during 2270-2299 period, we subtracted the initial active layer thickness (1960-1989 average) to 3 meters. Population Pearson correlations (*r*) significant at *p<0.01 and **p<2e-16.

3.3 Precipitation, ET, and Runoff

Models may project surface soil drying but the hydrological pathways through which this drying occurs appears to differ across models. The diversity of precipitation partitioning (Figure 5) demonstrates that specific representations and parameterizations for ET and runoff are not consistent across models. Though some models maintain a similar R/P ratio throughout the simulation (e.g., CLM, COLM, LPJGUESS), others show shifts from an ET-dominated system to a runoff-dominated system (e.g. JULES) and vice versa (e.g. TEM6 and UWVIC).

Evapotranspiration from the permafrost area is projected to rise in all models driven by warmer air temperatures and more productive vegetation, but the amplitude of that trend varies widely. The average projected evapotranspiration increase is 0.1±0.1mm/day (mean ± SD, hereafter) by 2100, which represents about a 25% increase over 20th century levels. Beyond 2100, the ET projections diverge (Figure 2e).

Runoff is also projected to increase with projections across models being highly variable (Figure 2g). The change in the models' ensemble mean between 1960-2299 was 0.2±0.2 mm/day. CLM, COLM, LPJGUESS and TEM6 simulated runoff changes of 0.2 to 0.3 mm/day by 2299. UWVIC exhibit small to null changes in runoff while SIBCASA shows surface runoff only.

Comparison between gauge station data and runoff simulations from the major river basins in the permafrost region shows that most models agree on the long term timing (Figure 6, Table 3) but the magnitude is generally underestimated (Figure 7). The gauge discharge mean for the four river basins is 219 ± 36 mm/yr compared to the models' ensemble mean of 101 ± 82 mm/yr for the period 1970-1999. Excluding SIBCASA, the models' ensemble mean is 134 ± 69 mm/yr. However, models show reasonable correlations between runoff output and observed annual discharge time series (Table 3). SIBCASA horizontal subsurface runoff was disabled on the simulation because it tended to drain the active layer completely, resulting in very low and unrealistic soil moisture. Therefore, SIBCASA runoff values shown in this study are only for surface runoff.

The net water balance (P-ET-R) is projected to increase for most models with precipitation increases outpacing the sum of ET and runoff changes. All models except TEM6 show an increase in the net water balance over the simulation period which suggests that models are collecting soil water deeper in the soil column, presumably in response to increasing ALT, even while the top soil layers dry.

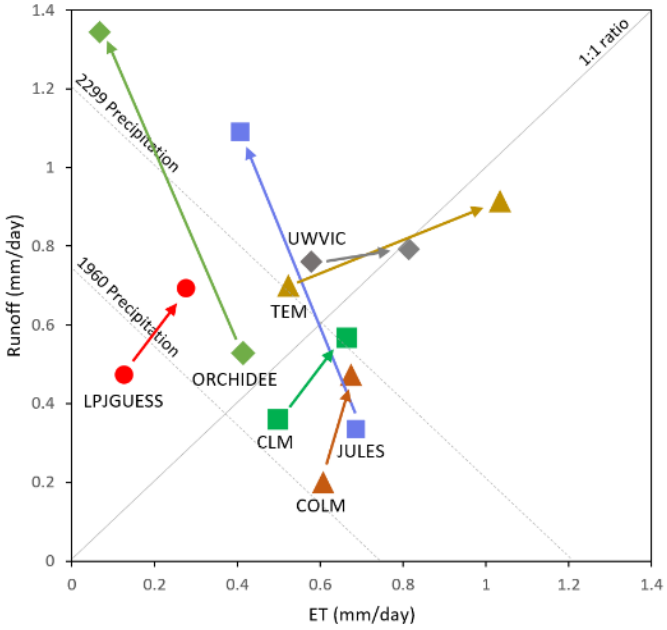

Figure 5. Precipitation partitioning between total runoff and evapotranspiration for participating models. Markers and arrows indicate the change from initial period (1960-1989 average) to final period (2270-2299 average). Diagonal dashed lines represent the ensemble rainfall mean for the initial (0.74 mm/day) and final (1.2 mm/day) simulation years. At any point along the dashed diagonals, runoff and ET sum to precipitation.

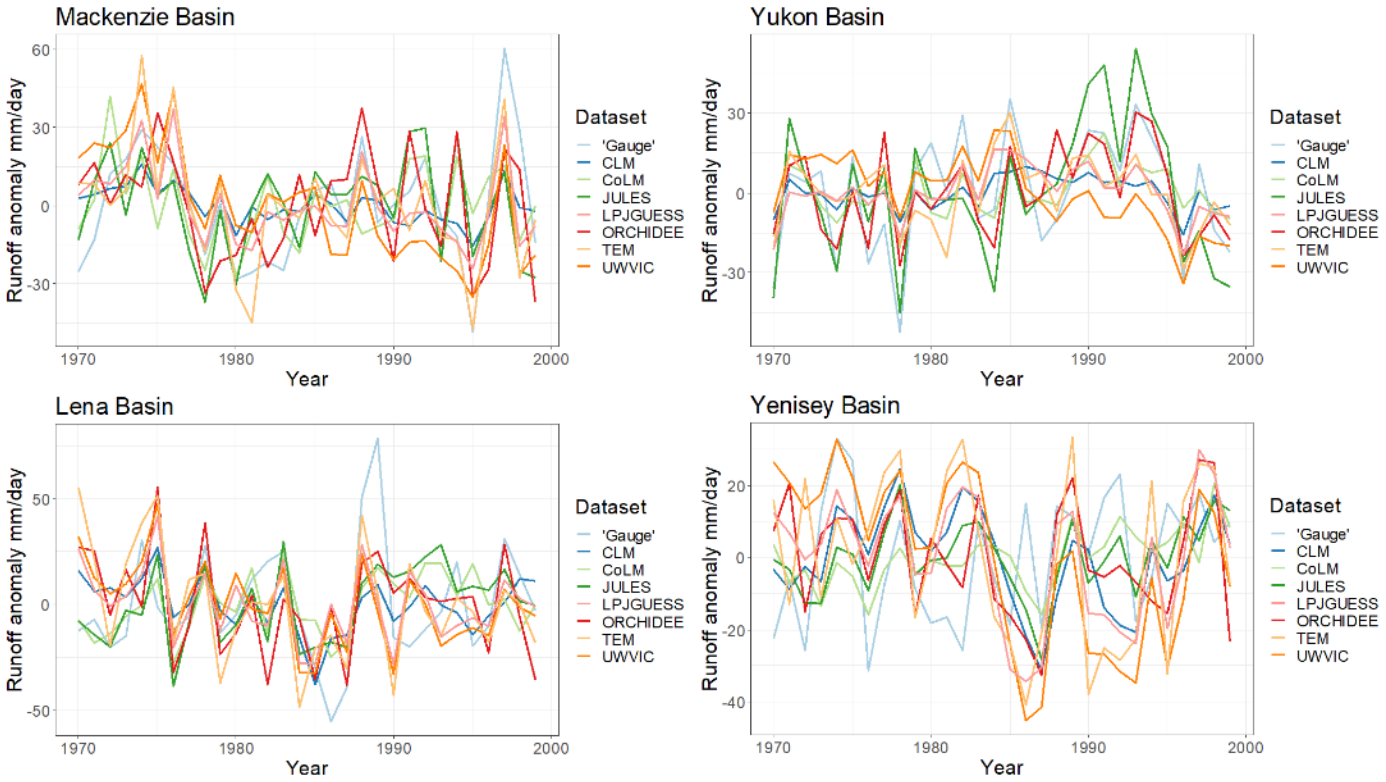

Figure 6. Runoff anomaly comparison between gauge data and models simulations for the period 1970-1999.

Table 3. Correlation coefficients between simulated annual total runoff and gauge mean annual discharge 1970 to 1999. SIBCASA correlations are for surface runoff.

	River Basin				
Model	Mackenzie	Yukon	Yenisey	Lena	Avg.
CLM	0.70	0.64	0.08	0.46	0.47
ORCHIDEE	0.57	0.69	0.36	0.37	0.50
LPJGGUESS	0.68	0.71	0.14	0.35	0.47
TEM	0.66	0.56	0.16	0.40	0.45
SIBCASA	0.49	0.21	0.08	0.29	0.27
JULES	0.41	0.77	0.34	0.51	0.51
COLM	0.38	0.76	0.27	0.46	0.47
UWVIC	0.44	0.38	0.02	0.31	0.29
Avg.	0.54	0.59	0.18	0.40	

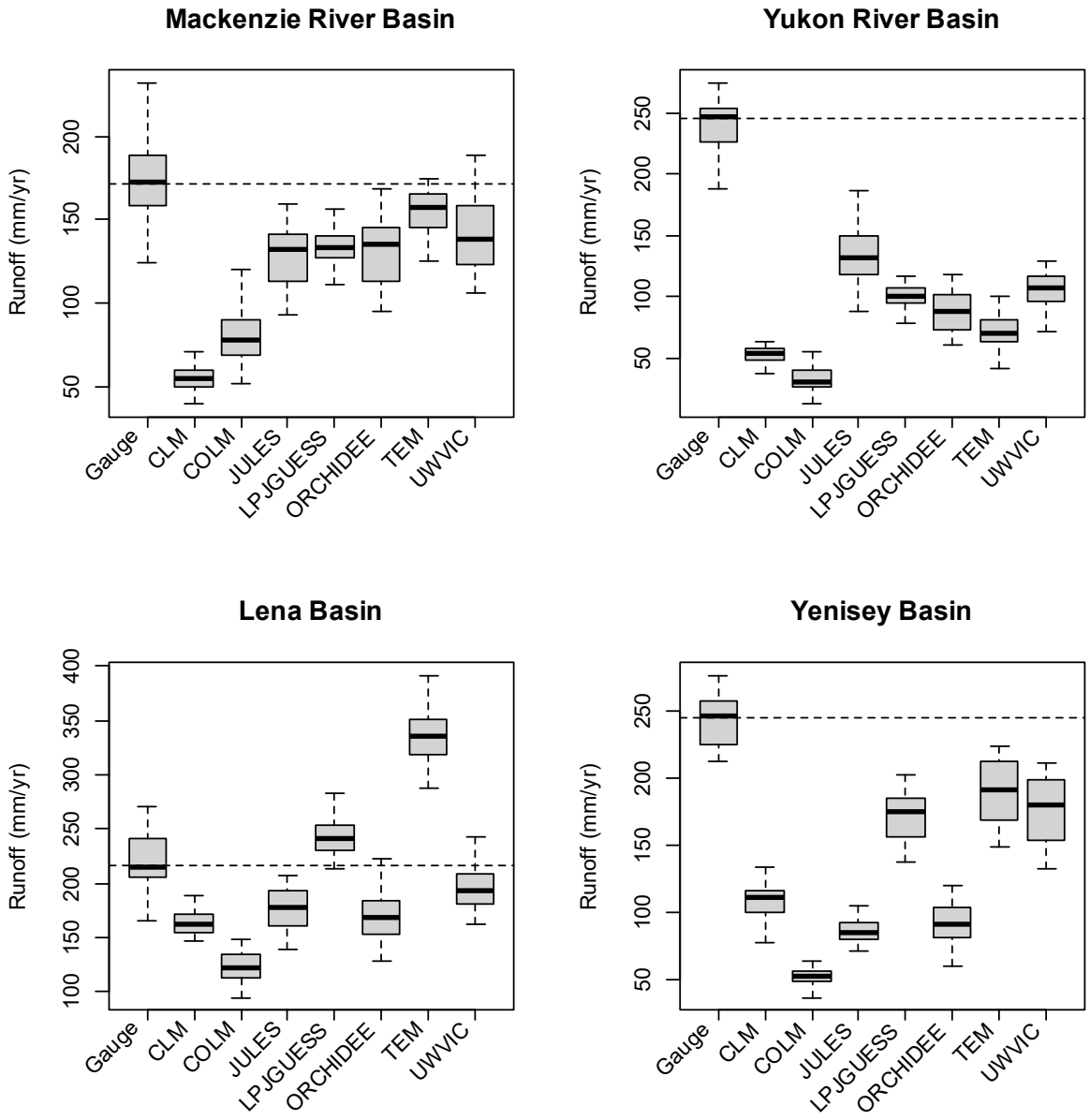

Figure 7. Discharge comparison between gauge station data and model output for each river basin. Dashed line indicates mean annual discharge at gauge station. Boxplots derived from mean annual discharge (total runoff) simulations for the period of 1970 to 1999.

4. Discussion

This study assessed near-surface soil moisture and hydrology projections in the permafrost region using widely-used land models that represent permafrost. Most models showed near-surface drying despite the externally-forced intensification of the water cycle driven by climate change. Drying was generally associated with increases of active layer thickness and permafrost degradation in a warming climate. We show that the timing and magnitude of projected soil moisture changes vary widely across models,

pointing to an uncertain future in permafrost hydrology and associated climatic feedbacks. In this section, we review the role of projected permafrost loss and active layer thickening on soil moisture changes and some potential sources of variability among models. In addition, we comment on the potential effects of soil moisture projections on the permafrost carbon-climate feedback. It is important to note that this study is more qualitative in nature and does not focus on the detail of magnitude or spatial patterns of model signatures.

4.1 Permafrost degradation and drying

Increases in net precipitation and the counterintuitive drying of the top soil in the permafrost region suggests that soil column processes such as changes in active layer thickness (ALT) and activation of subsurface drainage with permafrost thaw are acting to dry the top soil layers (Figure 8a). In general, models represent impermeable soils when frozen. Then, as soils thaw at progressively depths in the summer, liquid water infiltrates further into the active layer draining deeper into the thawed soil column (Avis et al., 2011; Lawrence et al., 2015; Swenson et al., 2012). However, relevant soil column processes related to thermokarst by thawing of excess ground ice (Lee et al., 2014) are limited in these simulations despite their significant occurrence in the permafrost region (Olefeldt et al., 2016). As permafrost thaws, ground ice melts, potentially reducing the volume of the soil column and changing the hydrological properties of the soil (Aas et al., 2019; Nitzbon et al., 2019). This would occur where soil surface elevation drops through sudden collapse or slow deformation by an amount equal to or greater than the increased depth of annual thaw (Figure 8b). This mechanism, not represented in current large-scale models, could result in projected increases or no change in the water table over time as observed by long-term studies (Andresen and Lougheed, 2015; Mauritz et al., 2017; Natali et al., 2015). Subsidence of 12-13 cm has been observed in Northern Alaska over a five year period, which represents a volume loss of about 25% of the average ALT for that region (~50cm) (Streletskiy et al., 2008). These lines of evidence may suggest that permafrost thaw may not dry the Arctic as fast as simulated by land models but rather maintain or enhanced soil water saturation depending on the water balance of the modeled cell column.

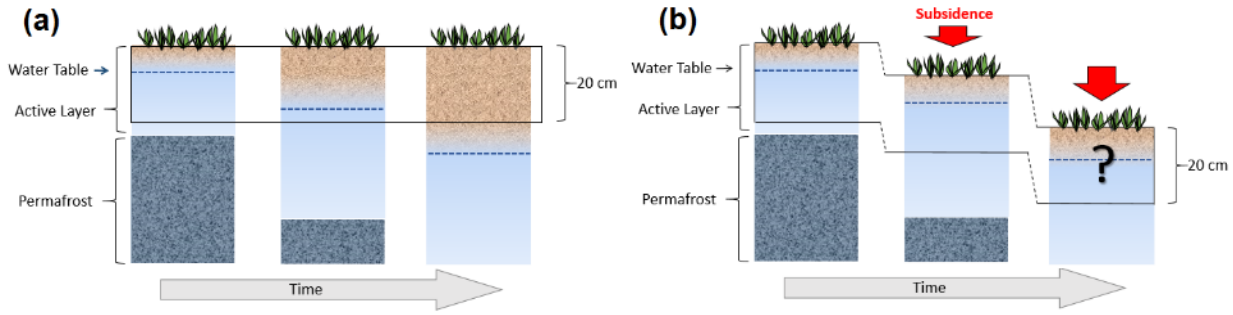

Figure 8. Schematic of changes in the soil column moisture (a) without subsidence (current models) and (b) with subsidence from thawing ice-rich permafrost (not represented by models), a process that may accumulate soil moisture and slow down drying over time.

Recent efforts have been made to address the high sub-grid heterogeneity of fine-scale mechanisms including soil subsidence (Aas et al., 2019), hillslope hydrology, talik and thermokarst development (Jafarov et al., 2018), ice wedge degradation (Abolt et al., 2018; Liljedahl et al., 2016; Nitzbon et al., 2019), vertical and lateral heat transfer on permafrost thaw and groundwater flow (Kurylyk et al., 2016)

and lateral water fluxes (Nitzbon et al., 2019). These processes are known to have a major role on surface and subsurface hydrology and their implementation in large scale models is needed. Other important challenges in land models' hydrology include representation of the significant area dynamics of the ubiquitous smaller, shallow water bodies observed over recent decades (Andresen and Lougheed, 2015; Jones et al., 2011; Roach et al., 2011; Smith et al., 2005). These systems are either lacking in simulations (polygon ponds and small lakes) or assumed to be static systems in simulations (large lakes). The implementation of surface hydrology dynamics and permafrost processes in large-scale land models will help reduce uncertainty in our ability to predict the future hydrological state of the Arctic and the associated climatic feedbacks. It is important to note that all these processes require data for model calibration, verification and evaluation, that is commonly absent at large scales. Permafrost hydrology will only advance through synergistic efforts between field researchers and modelers.

4.2 Uncertainty in soil moisture and hydrology simulations

Differences in representations of soil thermal dynamics can directly affect hydrology through timing of the freezing-thawing cycle and by altering the rates of permafrost loss and subsurface drainage (Finney et al., 2012). McGuire et al. (2016) and Peng et al. (2016) show that these models exhibit considerable differences in permafrost quantities such as active layer thickness, and the mean and trends in near-surface (0-3m) permafrost extent, even though all the models are forced with observed climatology. However, these differences are smaller than those seen across the CMIP5 models (Koven et al., 2013). All models except ORCHIDEE employ a multi-layer finite difference heat diffusion for soil thermal dynamics (Table 2). Organic soil insulation, snow insulation, and unfrozen water effects on phase change are the most common structural differences among models for soil thermal dynamics but do not explain the variability in the simulated changes in ALT and permafrost area as shown by McGuire *et al* (2016). Half of the participating models include organic matter in the soil properties (CLM, ORCHIDEE, SIBCASA, UWVIC) which can significantly impact soil thermal properties and lead to an increase in the hydraulic conductivity of the soil column, thereby enhancing drainage and redistribution of water in the soil column. Soil vertical characterization is another important aspect for soil thermal dynamics and hydrology (Chadburn et al., 2015; Nicolsky et al., 2007). Lawrence et al (2008) indicated that a high-resolution soil column representation is necessary for accurate simulation of long term trends in active layer depth. However, McGuire *et al* (2016) showed that soil column depth did not clearly explain variability of the simulated loss of permafrost area across models.

Water table representation can result in a first order effect on soil moisture. Most models (CLM, COLM, SIBCASA and ORCHIDEE) use some version of TOPMODEL (Niu et al., 2007), which employs a prognostic water table where sub-grid scale topography is the main driver of soil moisture variability in the cell. However, water table is not explicitly represented in other models such as LPJGUESS, which has a uniform water table which is only applied for wetland areas. In addition to water table, storage and transmission of water in soils is a fundamental component of an accurate representation of soil moisture (Niu and Yang, 2006). The representation of soil water storage and transmission varies across models from Richards equations based on Clapp Hornberger and/or van Genuchten (1980) functions (e.g CLM, CoLM, SIBCASA, ORCHIDEE) to a simplified one layer bucket (e.g. TEM6). It is also important to note that most models differ in their numerical implementations of processes, such as water movement through frozen soils (Gouttevin, I. et al., 2012; Swenson et al., 2012), and in the use of iterative solutions and vertical discretization of water transmission (De Rosnay et al., 2000).

Differences in representation of vertical fluxes through evapotranspiration (ET) are also likely adding to the high variability in soil moisture projections. ET sources (e.g. interception loss, plant transpiration, soil evaporation) were similar across models but had different formulations (Table 2). The diversity of ET implementations (e.g. evaporative resistances from fractional areas, etc.) and of vegetation maps used by the modelling groups (Ottlé et al., 2013) can also contribute to the big spread on the temporal simulations for ET and soil moisture. Along with projected increases in ET, net precipitation (P-ET) is projected to increase for all models suggesting that drying is not attributed only to soil evaporation, and the increasing net water balance (P-ET-R) proposes that models are storing water deeper in the soil column as permafrost near the surface thaws.

Despite runoff improvements (Swenson et al., 2012), underestimation of river discharge has been a challenge in previous versions in models (Slater et al., 2007). The differences between models and observations in mean annual discharge may stem from several sources. Particularly, the substantial variation in the precipitation forcing for these models (Figure 2e). This is attributed, in part, to the sparse observational networks in high latitudes. River discharge at high latitudes can differ substantially when different reanalysis forcing datasets are used. For example, river discharge for Arctic rivers differs substantially in CLM4.5 simulations when forced with GSWP3v1 compared to CRUNCEPv7 reanalysis datasets (not shown, runoff for MacKenzie, +32%; Yukon, +78%; Lena, -2%; Yenisey, +22%). Other factors include potential deficiencies in the parameterization and/or implementation of ET and runoff processes as well as vegetation processes.

4.3 Implications for the permafrost carbon-climate feedback

If drying of the permafrost region occurs, carbon losses from the soil will be dominated by CO_2 as a result of increased heterotrophic respiration rates compared to moist conditions (Elberling et al., 2013; Oberbauer et al., 2007; Schädel et al., 2016). With projected drying, CH_4 flux emissions will slow down by the reduction of soil saturation and inundated areas through lowering the water table in grid cells (Figure 8A). In a sensitivity study using CLM, the slower increase of methane emissions associated with surface drying could potentially lead to a reduction in the Global Warming Potential of permafrost carbon emissions by up to 50% compared to saturated soils (Lawrence et al., 2015). However, we need to also consider that current land models lack representation of important CH_4 sources and pathways in the permafrost region such as lake and wetland dynamics that can counteract the suppression of CH_4 fluxes by projected drying. Seasonal wetland area variation, which is not represented or is poorly represented in current models, can contribute to a third of the annual CH_4 flux in boreal wetlands (Ringeval et al., 2012). Although this manuscript may raise more questions than answers, this study highlights the importance of advancing hydrology and hydrological heterogeneity in land models to help determine the spatial variability, timing, and reasons for changes in hydrology of terrestrial landscapes of the Arctic. These improvements may constrain projections of land-atmosphere carbon exchange and reduce uncertainty on the timing and intensity of the permafrost carbon feedback.

Data availability

The simulation data analyzed in this manuscript is available through the National Snow and Ice Data Center (NSIDC; http://nsidc.org). Inquires please contact Kevin Schaefer (kevin.schaefer@nsidc.org).

Author contributions

This manuscript is a collective effort of the modeling groups of the Permafrost Carbon Network (http://www.permafrostcarbon.org). C.G.A, D.M.L., C.J.W., A.D.M. wrote the initial draft with additional contributions of all authors. Figures prepared by C.G.A.

Acknowledgements

This manuscript is dedicated to the memory of Andrew G. Slater (1971 -2016) for his scientific contributions in advancing Arctic hydrology modeling. This work was performed under the Next-Generation Ecosystem Experiments (NGEE Arctic, DOE ERKP757) project supported by the Office of Biological and Environmental Research in the U.S. Department of Energy, Office of Science. The study was also supported by the National Science Foundation through the Research Coordination Network (RCN) program and through the Study of Environmental Arctic Change (SEARCH) program in support of the Permafrost Carbon Network. We also acknowledge the joint DECC/Defra Met Office Hadley Centre Climate Programme (GA01101) and the European Union FP7-ENVIRONMENT project PAGE21.

References

Aas, K. S., Martin, L., Nitzbon, J., Langer, M., Boike, J., Lee, H., Berntsen, T. K. and Westermann, S.: Thaw processes in ice-rich permafrost landscapes represented with laterally coupled tiles in a land surface model, Cryosphere, 13(2), 591–609, doi:10.5194/tc-13-591-2019, 2019.

Abolt, C. J., Young, M. H., Atchley, A. L. and Harp, D. R.: Microtopographic control on the ground thermal regime in ice wedge polygons, Cryosphere, 12(6), 1957–1968, doi:10.5194/tc-12-1957-2018, 2018.

Andresen, C. G. and Lougheed, V. L.: Disappearing arctic tundra ponds: Fine-scale analysis of surface hydrology in drained thaw lake basins over a 65 year period (1948-2013)., J. Geophys. Res., 120, 1–14, doi:10.1002/2014JG002778, 2015.

Andresen, C. G., Lara, M. J., Tweedie, C. T. and Lougheed, V. L.: Rising plant-mediated methane emissions from arctic wetlands, Glob. Chang. Biol., 23(3), 1128–1139, doi:10.1111/gcb.13469, 2017.

Avis, C. a., Weaver, A. J. and Meissner, K. J.: Reduction in areal extent of high-latitude wetlands in response to permafrost thaw, Nat. Geosci., 4(7), 444–448, doi:10.1038/ngeo1160, 2011.

Best, M. J., Pryor, M., Clark, D. B., Rooney, G. G., Essery, R. L. H., Menard, C. B., Edwards, J. M., Hendry, M. a., Porson, a., Gedney, N., Mercado, L. M., Sitch, S., Blyth, E., Boucher, O., Cox, P. M., Grimmond, C. S. B. and Harding, R. J.: The Joint UK Land Environment Simulator (JULES), model description. Part 1: Energy and water fluxes, Geosci. Model Dev., 4, 677–699, doi:10.5194/gmdd-4-641-2011, 2011.

Bohn, T. J., Podest, E., Schroeder, R., Pinto, N., McDonald, K. C., Glagolev, M., Filippov, I., Maksyutov, S., Heimann, M., Chen, X. and Lettenmaier, D. P.: Modeling the large-scale effects of surface moisture heterogeneity on wetland carbon fluxes in the West Siberian Lowland, Biogeosciences, 10(10), 6559–6576, doi:10.5194/bg-10-6559-2013, 2013.

Bonan, G. B.: A Land Surface Model (LSM v1.0) for Ecological, Hydrological and Atmospheric studies: Technical descripton and user's guide., 1996.

Chadburn, S. E., Burke, E. J., Essery, R. L. H., Boike, J., Langer, M., Heikenfeld, M., Cox, P. M. and Friedlingstein, P.: Impact of model developments on present and future simulations of permafrost in a global land-surface model, Cryosphere, 9(4), 1505–1521, doi:10.5194/tc-9-1505-2015, 2015.

Dai, Y., Zeng, X., Dickinson, R. E., Baker, I., Bonan, G. B., Bosilovich, M. G., Denning, A. S., Dirmeyer P, Houser, P. R., Niu, G., Oleson, K. W., Schlosser, C. A. and Yang, Z.: The Common Land Model

(CoLM), Bull. Am. Meteorol. Soc., 84, 1013–1023, doi:10.1175/BAMS-84-8-1013, 2003.
Elberling, B., Michelsen, A., Schädel, C., Schuur, E. A. G., Christiansen, H. H., Berg, L., Tamstorf, M. P. and Sigsgaard, C.: Long-term CO2 production following permafrost thaw, Nat. Clim. Chang., 3(October), 890–894, doi:10.1038/nclimate1955, 2013.
Finney, D. L., Blyth, E. and Ellis, R. .: Improved modelling of Siberian river flow through the use of an alternative frozen soil hydrology scheme in a land surface model, Cryosph., 6, 859–870, doi:https://doi.org/10.5194/tc-6-859-2012, 2012.
Franccini, M. and Paciani, M.: Comparative analysis of several conceptual rainfall-runoff models, J. Hydrol., 122, 161–219, 1991.
Frey, K. E. and Mcclelland, J. W.: Impacts of permafrost degradation on arctic river biogeochemistry, Hydrol. Process., 23, 169–182, doi:10.1002/hyp, 2009.
Gent, P. R., Danabasoglu, G., Donner, L. J., Holland, M. M., Hunke, E. C., Jayne, S. R., Lawrence, D. M., Neale, R. B., Rasch, P. J., Vertenstein, M., Worley, P. H., Yang, Z. L. and Zhang, M.: The community climate system model version 4, J. Clim., 24(19), 4973–4991, doi:10.1175/2011JCLI4083.1, 2011.
Gerten, D., Schaphoff, S., Haberlandt, U., Lucht, W. and Sitch, S.: Terrestrial vegetation and water balance — hydrological evaluation of a dynamic global vegetation model, , 286, 249–270, doi:10.1016/j.jhydrol.2003.09.029, 2004.
Gouttevin, I., Krinner, G., Ciais, P., Polcher, J. and Legout, C.: Multi-scale validation of a new soil freezing scheme for a land-surface model with physically-based hydrology, Cryosph., 6, 407–430, 2012.
Grosse, G., Jones, B. and Arp, C.: Thermokarst lakes, drainage, and drained basins, in Treatise on Geomorphology, vol. 8, pp. 325–353., 2013.
Harris, I., Jones, P. D., Osborn, T. J. and Lister, D. H.: Updated high-resolution grids of monthly climatic observations - the CRU TS3.10 Dataset, Int. J. Climatol., 34(3), 623–642, doi:10.1002/joc.3711, 2014.
Haxeltine, A. and Prentice, I. C.: A General Model for the Light-Use Efficiency of Primary Production, Funct. Ecol., 10(5), 551–561, 1996.
Hayes, D. J., Mcguire, A. D., Kicklighter, D. W., Gurney, K. R., Burnside, T. J. and Melillo, J. M.: Is the northern high - latitude land - based CO 2 sink weakening ?, Global Biogeochem. Cycles, 25(May), 1–14, doi:10.1029/2010GB003813, 2011.
Hayes, D. J., Kicklighter, D. W., McGuire, a D., Chen, M., Zhuang, Q., Yuan, F., Melillo, J. M. and Wullschleger, S. D.: The impacts of recent permafrost thaw on land–atmosphere greenhouse gas exchange, Environ. Res. Lett., 9(4), 045005, doi:10.1088/1748-9326/9/4/045005, 2014.
Jafarov, E. and Schaefer, K.: The importance of a surface organic layer in simulating permafrost thermal and carbon dynamics, Cryosph., 10, 465–475, doi:10.5194/tc-10-465-2016, 2016, 2016.
Jafarov, E. E., Coon, E. T., Harp, D. R., Wilson, C. J., Painter, S. L., Atchley, A. L. and Romanovsky, V. E.: Modeling the role of preferential snow accumulation in through talik development and hillslope groundwater flow in a transitional permafrost landscape, Environ. Res. Lett., 13(10), doi:10.1088/1748-9326/aadd30, 2018.
Jensen, M. E. and Haise, H. R.: Estimating evapotranspiration from solar radiation, J. Irrig. Drain. Div. ASCE, (89), 15–41, 1963.
Ji, D., Wang, L., Feng, J., Wu, Q., Cheng, H., Q, Z., Yang, J., Dong, W., Dai, Y., Gong, D., Zhang, R. H., Wang, X., Liu, J., Moore, J. C., Chen, D. and Zhou, M.: Description and basic evaluation of Beijing Normal University Earth system model (BNU-ESM) version 1, Geosci. Model Dev., 7, 2039–2064, 2014.
Jones, B. M., Grosse, G., Arp, C. D., Jones, M. C., Walter Anthony, K. M. and Romanovsky, V. E.: Modern thermokarst lake dynamics in the continuous permafrost zone, northern Seward Peninsula, Alaska, J. Geophys. Res., 116, G00M03, doi:10.1029/2011JG001666, 2011.
Kanevskiy, M., Shur, Y., Jorgenson, T., Brown, D. R. N., Moskalenko, N., Brown, J., Walker, D. A., Raynolds, M. K. and Buchhorn, M.: Degradation and stabilization of ice wedges: Implications for assessing risk of thermokarst in northern Alaska, Geomorphology, 297, 20–42, doi:10.1016/j.geomorph.2017.09.001, 2017.
Koven, C., Friedlingstein, P., Ciais, P., Khvorostyanov, D., Krinner, G. and Tarnocai, C.: On the

519 formation of high-latitude soil carbon stocks: Effects of cryoturbation and insulation by organic matter in
520 a land surface model, Geophys. Res. Lett., 36(21), 1–5, doi:10.1029/2009GL040150, 2009.
521 Koven, C. D., Riley, W. J. and Stern, A.: Analysis of permafrost thermal dynamics and response to
522 climate change in the CMIP5 earth system models, J. Clim., 26(6), 1877–1900, doi:10.1175/JCLI-D-12-
523 00228.1, 2013.
524 Koven, C. D., Lawrence, D. M. and Riley, W. J.: Permafrost carbon−climate feedback is sensitive to deep
525 soil carbon decomposability but not deep soil nitrogen dynamics, Proc. Natl. Acad. Sci., 201415123,
526 doi:10.1073/pnas.1415123112, 2015.
527 Krinner, G., Viovy, N., de Noblet-Ducoudré, N., Ogée, J., Polcher, J., Friedlingstein, P., Ciais, P., Sitch,
528 S. and Prentice, I. C.: A dynamic global vegetation model for studies of the coupled atmosphere-
529 biosphere system, Global Biogeochem. Cycles, 19(1), 1–33, doi:10.1029/2003GB002199, 2005.
530 Kurylyk, B. L., Hayashi, M., Quinton, W. L., McKenzie, J. M. and Voss, C. I.: Influence of vertical and
531 lateral heat transfer on permafrost thaw, peatland landscape transition, and groundwater flow, Water
532 Resour. Res., 52(2), 1286–1305, doi:10.1002/2015WR018057, 2016.
533 Lara, M. J., McGuire, A. D., Euskirchen, E. S., Tweedie, C. E., Hinkel, K. M., Skurikhin, A. N.,
534 Romanovsky, V. E., Grosse, G., Bolton, W. R. and Genet, H.: Polygonal tundra geomorphological change
535 in response to warming alters future CO 2 and CH 4 flux on the Barrow Peninsula, Glob. Chang. Biol.,
536 21, 1663–1651, doi:10.1111/gcb.12757, 2015.
537 Lawrence, D. M., Slater, A. G., Romanovsky, V. E. and Nicolsky, D. J.: Sensitivity of a model projection
538 of near-surface permafrost degradation to soil column depth and representation of soil organic matter, J.
539 Geophys. Res., 113(F2), F02011, doi:10.1029/2007JF000883, 2008.
540 Lawrence, D. M., Koven, C. D., Swenson, S. C., Riley, W. J. and Slater, A. G.: Permafrost thaw and
541 resulting soil moisture changes regulate projected high-latitude CO_2 and CH_4 emissions, Environ. Res.
542 Lett., 10(9), 094011, doi:10.1088/1748-9326/10/9/094011, 2015.
543 Lee, H., Swenson, S. C., Slater, A. G. and Lawrence, D. M.: Effects of excess ground ice on projections
544 of permafrost in a warming climate, Environ. Res. Lett., 9(12), 124006, doi:10.1088/1748-
545 9326/9/12/124006, 2014.
546 Liang, X., Lettenmaier, D. P., Wood, E. F. and Burges, S.: A simple hydrologically based model of land
547 surface water and energy fluxes for general circulation models, J. Geophys. Res., 99(D7), 14415–14418,
548 1994.
549 Liljedahl, A., Boike, J., Daanen, R. P., Fedorov, A. N., Frost, G. V., Grosse, G., Hinzman, L. D., Iijma,
550 Y., Jorgenson, J. C., Matveyeva, N., Necsoiu, M., Raynolds, M. K., Romanovsky, V., Schulla, J., Tape,
551 K. D., Walker, D. A., Wilson, C., Yabuki, H. and Zona, D.: Pan-Arctic ice-wedge degradation in warming
552 permafrost and influence on tundra hydrology, Nat. Geosci., 9(April), 312–319, doi:10.1038/ngeo2674,
553 2016.
554 Mauritz, M., Bracho, R., Celis, G., Hutchings, J., Natali, S. M., Pegoraro, E., Salmon, V. G., Schädel, C.,
555 Webb, E. E. and Schuur, E. A. G.: Nonlinear CO2 flux response to 7 years of experimentally induced
556 permafrost thaw, Glob. Chang. Biol., 23(9), 3646–3666, doi:10.1111/gcb.13661, 2017.
557 McGuire, A. D., Lawrence, D. M., Koven, C., Clein, J. S., Burke, E., Chen, G., Jafarov, E., MacDougall,
558 A. H., Marchenko, S., Nicolsky, D., Peng, S., Rinke, A., Ciais, P., Gouttevin, I., Hayes, D. J., Ji, D.,
559 Krinner, G., Moore, J. C., Romanovsky, V., Schädel, C., Schaefer, K., Schuur, E. A. G. and Zhuang, Q.:
560 The Dependence of the Evolution of Carbon Dynamics in the Northern Permafrost Region on the
561 Trajectory of Climate Change, Proc. Natl. Acad. Sci., 2018.
562 McGuire, D. A., Koven, C. D., Lawrence, D. M., Burke, E., Chen, G., Chen, X., Delire, C. and Jafarov,
563 E.: Variability in the sensitivity among model simulations of permafrost and carbon dynamics in the
564 permafrost region between 1960 and 2009, Global Biogeochem. Cycles, 1–23,
565 doi:10.1002/2016GB005405.Received, 2016.
566 Mitchell, T. D. and Jones, P. D.: An improved method of constructing a database of monthly climate
567 observations and associated high-resolution grids, Int. J. Climatol., 25(6), 693–712, doi:10.1002/joc.1181,
568 2005.
569 Natali, S. M., Schuur, E. a G., Mauritz, M., Schade, J. D., Celis, G., Crummer, K. G., Johnston, C.,

570 Krapek, J., Pegoraro, E., Salmon, V. G. and Webb, E. E.: Permafrost thaw and soil moisture driving CO2
571 and CH4 release from upland tundra, J. Geophys. Res. Biogeosciences, 120, 525–537,
572 doi:10.1002/2014JG002872.Received, 2015.
573 Newman, B. D., Throckmorton, H. M., Graham, D. E., Gu, B., Hubbard, S. S., Liang, L., Wu, Y.,
574 Heikoop, J. M., Herndon, E. M., Phelps, T. J., Wilson, C. J. and Wullschleger, S. D.: Microtopographic
575 and depth controls on active layer chemistry in Arctic polygonal ground, Geophys. Res. Lett., 42(6),
576 1808–1817, doi:10.1002/2014GL062804, 2015.
577 Nicolsky, D. J., Romanovsky, V. E., Alexeev, V. A. and Lawrence, D. M.: Improved modeling of
578 permafrost dynamics in a GCM land-surface scheme, Geophys. Res. Lett., 34,
579 doi:10.1029/2007GL029525, 2007.
580 Nitzbon, J., Langer, M., Westerman, S., Martin, L., Schanke Aas, K. and Boike, J.: Modelling the
581 degradation of ice-wedges in polygonal tundra under different hydrological conditions, Cryosph., 13,
582 1089–1123, 2019.
583 Niu, G.-Y., Yang, Z.-L., Dickinson, R. E., Gulden, L. E. and Su, H.: Development of a simple
584 groundwater model for use in climate models and evaluation with Gravity Recovery and Climate
585 Experiment data, J. Geophys. Res., 112(D7), D07103, doi:10.1029/2006JD007522, 2007.
586 Niu, G. and Yang, Z.: Effects of Frozen Soil on Snowmelt Runoff and Soil Water Storage at a
587 Continental Scale, J. Hydrometeorol., 7, 937–952, doi:10.1175/JHM538.1, 2006.
588 Oberbauer, S., Tweedie, C., Welker, J. M., Fahnestock, J. T., Henry, G. H. R., Webber, P. J., Hollister, R.
589 D., Walker, D. A., Kuchy, A., Elmore, E. and Starr, G.: Tundra CO2 fluxes in response to experimental
590 warming across latitudinal and moisture gradients, Ecol. …, 77(2), 221–238 [online] Available from:
591 http://www.esajournals.org/doi/abs/10.1890/06-0649 (Accessed 10 July 2014), 2007.
592 Olefeldt, D., Goswami, S., Grosse, G., Hayes, D., Hugelius, G., Kuhry, P., Mcguire, A. D., Romanovsky,
593 V. E., Sannel, A. B. K., Schuur, E. A. G. and Turetsky, M. R.: Circumpolar distribution and carbon
594 storage of thermokarst landscapes, Nat. Commun., 7, 1–11, doi:10.1038/ncomms13043, 2016.
595 Oleson, K., Lawrence, D., Bonan, G., Drewniak, B., Huang, M., Koven, C., Levis, S., Li, F., Riley, W.,
596 Subin, Z., Swenson, S., Thornton, P., Bozbiyik, A., Fisher, R., Heald, C., Kluzek, E., Lamarque, J.-F.,
597 Lawrence, P., Leung, L., Lipscomb, W., Muszala, S., Ricciuto, D., Sacks, W., Sun, Y., Tang, J. and Yang,
598 Z.-L.: Technical description of version 4.5 of the Community Land Model (CLM), Boulder, Colorado.
599 [online] Available from: http://opensky.library.ucar.edu/collections/TECH-NOTE-000-000-000-870,
600 2013.
601 Ottlé, C., Lescure, J., Maignan, F., Poulter, B., Wang, T. and Delbart, N.: Use of various remote sensing
602 land cover products for plant functional type mapping over Siberia., Earth Syst. Sci. Data, 5(2), 331,
603 2013.
604 Peng, S., Ciais, P., Krinner, G., Wang, T., Gouttevin, I., McGuire, A. D., Lawrence, D., Burke, E., Chen,
605 X., Delire, C., Koven, C., MacDougall, A., Rinke, A., Saito, K., Zhang, W., Alkama, R., Bohn, T. J.,
606 Decharme, B., Hajima, T., Ji, D., Lettenmaier, D. P., Miller, P. A., Moore, J. C., Smith, B. and Sueyoshi,
607 T.: Simulated high-latitude soil thermal dynamics during the past four decades, Cryosph. Discuss., 9(2),
608 2301–2337, doi:10.5194/tcd-9-2301-2015, 2015.
609 Rawlins, M. a., Steele, M., Holland, M. M., Adam, J. C., Cherry, J. E., Francis, J. a., Groisman, P. Y.,
610 Hinzman, L. D., Huntington, T. G., Kane, D. L., Kimball, J. S., Kwok, R., Lammers, R. B., Lee, C. M.,
611 Lettenmaier, D. P., McDonald, K. C., Podest, E., Pundsack, J. W., Rudels, B., Serreze, M. C.,
612 Shiklomanov, A., Skagseth, Ø., Troy, T. J., Vörösmarty, C. J., Wensnahan, M., Wood, E. F., Woodgate,
613 R., Yang, D., Zhang, K. and Zhang, T.: Analysis of the Arctic System for Freshwater Cycle
614 Intensification: Observations and Expectations, J. Clim., 23(21), 5715–5737,
615 doi:10.1175/2010JCLI3421.1, 2010.
616 Ringeval, B., Decharme, B., Piao, S. L., Ciais, P., Papa, F., De Noblet-Ducoudré, N., Prigent, C.,
617 Friedlingstein, P., Gouttevin, I., Koven, C. and Ducharne, a.: Modelling sub-grid wetland in the
618 ORCHIDEE global land surface model: Evaluation against river discharges and remotely sensed data,
619 Geosci. Model Dev., 5, 941–962, doi:10.5194/gmd-5-941-2012, 2012.
620 Roach, J., Griffith, B., Verbyla, D. and Jones, J.: Mechanisms influencing changes in lake area in Alaskan

boreal forest, Glob. Chang. Biol., 17(8), 2567–2583, doi:10.1111/j.1365-2486.2011.02446.x, 2011.
De Rosnay, P. and Polcher, J.: Modelling root water uptake in a complex land surface scheme coupled to a GCM, Hydrol. Earth Syst. Sci., 2(2/3), 239–255, doi:10.5194/hess-2-239-1998, 1998.
De Rosnay, P., Bruen, M. and Polcher, J.: Sensitivity of surface fluxes to the number of layers in the soil model used in GCMs, Geophys. Res. Lett., 27(20), 3329–3332, doi:10.1029/2000GL011574, 2000.
Schädel, C., Bader, M. K.-F., Schuur, E. A. G., Biasi, C., Bracho, R., Čapek, P., De Baets, S., Diáková, K., Ernakovich, J., Estop-Aragones, C., Graham, D. E., Hartley, I. P., Iversen, C. M., Kane, E., Knoblauch, C., Lupascu, M., Martikainen, P. J., Natali, S. M., Norby, R. J., O'Donnell, J. A., Chowdhury, T. R., Šantrůčková, H., Shaver, G., Sloan, V. L., Treat, C. C., Turetsky, M. R., Waldrop, M. P. and Wickland, K. P.: Potential carbon emissions dominated by carbon dioxide from thawed permafrost soils, Nat. Clim. Chang., 6(10), 950–953, doi:10.1038/nclimate3054, 2016.
Schaefer, K., Zhang, T., Bruhwiler, L. and Barrett, A. P.: Amount and timing of permafrost carbon release in response to climate warming, Tellus, Ser. B Chem. Phys. Meteorol., 63(2), 165–180, doi:10.1111/j.1600-0889.2011.00527.x, 2011.
Sheffield, J., Goteti, G. and Wood, E. F.: Development of a 50-year high-resolution global dataset of meteorological forcings for land surface modeling, J. Clim., 19(13), 3088–3111, doi:10.1175/JCLI3790.1, 2006.
Slater, A. G. and Lawrence, D. M.: Diagnosing present and future permafrost from climate models, J. Clim., 26(15), 5608–5623, doi:10.1175/JCLI-D-12-00341.1, 2013.
Slater, A. G., Bohn, T. J., McCreight, J. L., Serreze, M. C. and Lettenmaier, D. P.: A multimodel simulation of pan-Arctic hydrology, J. Geophys. Res. Biogeosciences, 112(4), 1–17, doi:10.1029/2006JG000303, 2007.
Smith, L. C., Sheng, Y., MacDonald, G. M. and Hinzman, L. D.: Disappearing Arctic lakes., Science, 308(5727), 1429, doi:10.1126/science.1108142, 2005.
Streletskiy, D. A., Shiklomanov, N. I., Nelson, F. E. and Klene, A. E.: 13 Years of Observations at Alaskan CALM Sites : Long-term Active Layer and Ground Surface Temperature Trends, in Ninth International Conference on Permafrost, edited by D. L. Kane and K. M. Hinkel, pp. 1727–1732, University of Alaska at Fairbanks, Fairbanks, AK., 2008.
Swenson, S. C., Lawrence, D. M. and Lee, H.: Improved simulation of the terrestrial hydrological cycle in permafrost regions by the Community Land Model, J. Adv. Model. Earth Syst., 4(8), 1–15, doi:10.1029/2012MS000165, 2012.
Thornthwaite, C. and Mather, J. R.: Instructions and tables for computing potential evapotranspiration and the water balance: Centeron, N.J., Laboratory of Climatology., Publ. Climatol., 10(3), 185–311, 1957.
Throckmorton, H. M., Heikoop, J. M., Newman, B. D., Altmann, G. L., Conrad, M. S., Muss, J. D., Perkins, G. B., Smith, L. J., Torn, M. S., Wullschleger, S. D. and Wilson, C. J.: Pathways and transformations of dissolved methane and dissolved inorganic carbon in Arctic tundra watersheds: Evidence from analysis of stable isotopes, Global Biogeochem. Cycles, 29, 1893–1910, doi:10.1002/2014GB005044.Received, 2015.
Walvoord, M. A. and Kurylyk, B. L.: Hydrologic Impacts of Thawing Permafrost—A Review, Vadose Zo. J., 15(6), 0, doi:10.2136/vzj2016.01.0010, 2016.
Wang, W., Rinke, A., Moore, J. C., Ji, D., Cui, X., Peng, S., Lawrence, D. M., McGuire, A. D., Burke, E. J., Chen, X., Decharme, B., Koven, C., MacDougall, A., Saito, K., Zhang, W., Alkama, R., Bohn, T. J., Ciais, P., Delire, C., Gouttevin, I., Hajima, T., Krinner, G., Lettenmaier, D. P., Miller, P. A., Smith, B., Sueyoshi, T. and Sherstiukov, A. B.: Evaluation of air-soil temperature relationships simulated by land surface models during winter across the permafrost region, Cryosphere, 10(4), 1721–1737, doi:10.5194/tc-10-1721-2016, 2016.
Wania, R., Ross, I. and Prentice, I. C.: Integrating peatlands and permafrost into a dynamic global vegetation model : 1 . Evaluation and sensitivity of physical land surface processes, , 23, 1–19, doi:10.1029/2008GB003412, 2009a.
Wania, R., Ross, I. and Prentice, I. C.: Integrating peatlands and permafrost into a dynamic global vegetation model : 2 . Evaluation and sensitivity of vegetation and carbon cycle processes, , 23, 1–15,

doi:10.1029/2008GB003413, 2009b.
Willmott, C. J. and Matsuura, K.: Terrestrial air temperature and precipitation: Monthly and annual time series (1950–1999) Version 1.02., 2001.